Combinatorial models of global dynamics: learning cycling motion from data

Ulrich Bauer*, David Hien*, Oliver Junge*, Konstantin Mischaikow † and Max Snijders ‡
*Department of Mathematics, Technical University of Munich, Germany
†Department of Mathematics, Rutgers University, Piscataway, NJ, USA
‡Boston Consulting Group

Summary. We describe a computational method for constructing a coarse combinatorial model of a dynamical system in which the macroscopic states are given by elementary cycling motions of the system. Our method is based on tools from topological data analysis and can be applied to time series data. We illustrate the construction by a perturbed double well Hamiltonian as well as the Lorenz system.

Introduction

Conley's fundamental theorem [4] characterizes the global structure of the dynamics of a continuous map on a compact metric space. It states that the space can be decomposed into a (chain) recurrent set and its complement, on which the map behaves gradient-like, i.e. trajectories transit from one recurrent component to another. Around the turn of the century, a computational approach to this theory has been developed [12, 7, 9, 10, 1, 11].
Relatedly, ideas have been put forward in order to characterize the dynamics *within* a transitive component of the chain recurrent set. For example, in [6], certain eigenfunctions of the transfer (or push forward) operator have been used in order to decompose a transitive component into, e.g., *almost invariant* (or metastable) subsets.
The purpose of this note is to outline a computational procedure by which certain *cycling behaviour* of the system can be detected and agglomerated into a coarse model. More precisely, we describe how to detect whether the system exhibits motions along a topological circle in some geometric complex that represents a transitive recurrent component of the system. A key ingredient in this procedure is a construction of circle-valued coordinates on simplicial complexes [5]; its usefulness for analyzing recurrent dynamics was already suggested in [14].
In particular, our technique is applicable if no model is available, but the dynamics is only given in form of a time series of data points $x_k = x(t_k) \in \mathbb{R}^d$, $k = 0, \dots, m$, that are, e.g., sampled from solution curves $x : [0, 1] \to \mathbb{R}^d$ of some differential equation or constructed by a time-delay embedding of scalar measurement data.

The construction

Given a time series $x_0, \dots, x_m$ in $\mathbb{R}^d$, we construct a combinatorial model which captures different types of cycling motion. Our pipeline consists of three main steps: constructing a topological space, finding dynamically relevant coordinates and constructing a combinatorial model.

Discretization of phase space

A first attempt at obtaining a topological space from a time series $x_0, \dots, x_m$ is to construct a Vietoris–Rips complex with base set $X = \{x_0, \dots, x_m\}$. In our setting, this is impractical since the resulting complexes are usually too large to be computationally tractable. In order to circumvent this problem we first quantize our data. For this, choose a radius $r \in \mathbb{R}_{>0}$ and consider the *cubical grid*

$$\mathcal{B} = \mathcal{B}(r) = \left\{ \prod_{\ell=1}^{d} r\left[z_\ell - \tfrac{1}{2}, z_\ell + \tfrac{1}{2}\right) \mid z \in \mathbb{Z}^d \right\}.$$

Since the elements of $\mathcal{B}$ (which we call *cubes* or *boxes*) form a partition of $\mathbb{R}^d$, we can define $Q : \mathbb{R}^d \to \mathcal{B}$ by mapping each point to the unique cube containing the point. Then

$$\mathcal{X} := \{Q(x) \mid x \in X\}$$

is a *cubical* or *box covering* of the point cloud X. For a cube $\xi = \prod_{\ell=1}^{d} r\left[z_\ell - \frac{1}{2}, z_\ell + \frac{1}{2}\right)$ let $z(\xi) = (rz_1, \dots, rz_d)$ be its *center*. We can identify $\mathcal{X}$ with the subset

$$Z := \{z(\xi) \mid \xi \in \mathcal{X}\}$$

of the integer lattice $r\mathbb{Z}^d$. The set Z of box centers is called the *quantization of the point cloud* X. Fig. 1a shows a time series with its cubical cover and the corresponding set of box centers Z.
We then resample the time series such that consecutive points lie in different cubes. For this, set $\tau(0) = 0$ and recursively define

$$\tau(i) = \min\{j > \tau(i-1) \mid Q(x_j) \neq Q(x_{\tau(i-1)})\}$$

The time series $\hat{x}_i = z \circ Q(x_{\tau(i)})$, $i \in [0, T]$ is called the *quantization* of the time series $x_0, \dots, x_m$ at radius r. Here we let T denote the largest finite value of τ and $[k, \ell] := \{k, \dots, \ell\} \subset \mathbb{N}_0$.

(a) Time series and cubical quantization.

(b) Vietoris–Rips complex

Figure 1: Time series, its quantization and the resulting Vietoris–Rips complex.

Given a set of box centers Z, we construct the Vietoris–Rips complex $\mathcal{K} = \mathrm{VR}(Z, d, \delta)$, where $d(x, y) = \|x - y\|_\infty$ and $\delta = r$ (see the appendix for a definition of the Vietoris–Rips complex). Note that the choice of d and δ allows a point in Z to be connected to all its diagonal neighbors. An example is shown in Fig. 1b.

Coordinates for dynamics

Circular coordinates are the key tool which we use to detect cycling. In the following paragraphs, we review their construction from cohomology, explain how they can be lifted with respect to a time series, and outline how to find elements of $H^1(\mathcal{K}; \mathbb{Z})$ that induce dynamically relevant coordinates. In particuar, we will also define what it means to be cycling with respect to a coordinate.

1. Cohomology and circular coordinates. A circular coordinate, as introduced in [5], is a function $\mathcal{K} \to S^1$ with minimal variation along edges in its homotopy class (in particular, there is no relation to coordinates in the sense of differential geometry). Abstractly, the construction of circular coordinates is motivated by the bijection $H^1(\mathcal{K}; \mathbb{Z}) \cong [\mathcal{K}, S^1]$ where $[\mathcal{K}, S^1]$ denotes the homotopy classes of maps $\mathcal{K} \to S^1$. Explicitly, given a cocycle $\alpha \in Z^1(\mathcal{K}; \mathbb{Z})$, the coordinate $\theta_\alpha : \mathcal{K} \to S^1$ can be constructed by first computing the *harmonic representative* which is given by

$$\operatorname{argmin}\{\|\bar{\alpha}\|^2 \mid \bar{\alpha} = \alpha + d_0\theta, \theta \in C^0(\mathcal{K}; \mathbb{R})\}, \quad \text{where } \|\alpha\|^2 = \sum_{e \in \mathcal{K}^1} \alpha(e)^2,$$

and then using the construction from [5] to obtain a function $\mathcal{K} \to S^1$ which "varies by $\bar{\alpha}(e)$ on each edge e". In this work, the precise construction is not important since we only use the values of this function on the vertices of $\mathcal{K}$ which is given by composing the minimizing θ with the canonical projection $\pi_{S^1} : \mathbb{R} \to S^1 = \mathbb{R}/\mathbb{Z}$. We denote this function by $\theta_\alpha : Z \to S^1$. We remark that θ_α only depends on the cohomology class of α and is unique up to an additive constant on each connected component of $\mathcal{K}$. Examples can be found in Figs. 2 and 3.

(a) Coordinate θ_α varies around the right hole.

(b) Coordinate θ_β varies around the left hole.

Figure 2: Circular coordinates which capture holes in the complex.

2. Lifted coordinates. Given a quantized time series $\hat{x} : [0, T] \to Z$ and a circular coordinate $\theta : Z \to S^1$ we can form the composite $\theta \circ \hat{x} : [0, T] \to S^1$ which captures the change of the coordinate θ over time. Analogous to continuous maps, we lift this function to a function $\hat{\theta} : [0, T] \to \mathbb{R}$ such that $\pi_{S^1} \circ \hat{\theta} = \theta \circ \hat{x}$: We define the *lifted coordinate* of θ and $\hat{x}$ via $\hat{\theta}(0) = 0$ and

$$\hat{\theta}(t) = \hat{\theta}(t-1) + d_{S^1}(\theta(\hat{x}_t), \theta(\hat{x}_{t-1})), \quad t = 1, \ldots, T,$$

where $d_{S^1}(x, y)$ denotes the signed geodesic distance from y to x on S^1.
For an example, let $\hat{x}$ denote the quantized time setries from Fig. 1a. Fig. 4a shows the first 80 time steps of $\theta_\alpha \circ \hat{x}$, Fig.4b shows the lift $\hat{\theta}$ over the same period of time. One can see from Fig. 4a that the time series does approximately 3.5 turns with respect to the coordinate. The lifted coordinate Fig. 4b captures this directly, as it increases by 3.5.

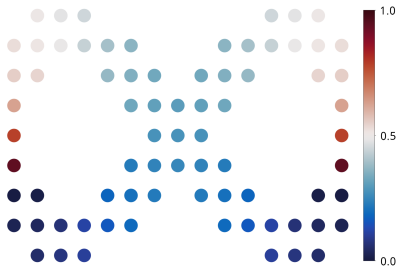

(a) Coordinate θ_γ varies around both holes.

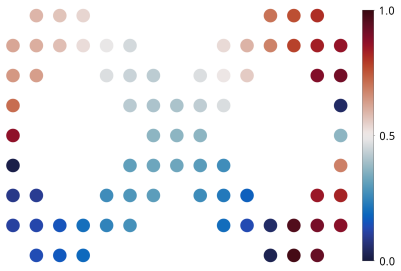

(b) Coordinate θ_δ varies around both holes.

Figure 3: A pair of bad coordinates.

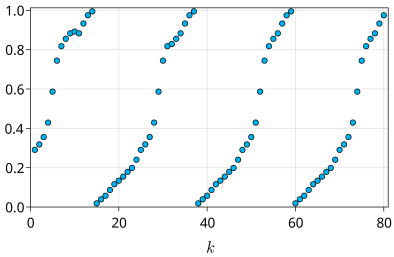

(a) Circular coordinate evaluated along time series.

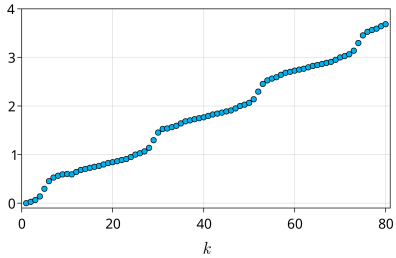

(b) Lifted coordinate.

Figure 4: Circular coordinate and its lift along a time series.

3. Dynamically relevant generators. As described before, every cohomology class in $H^1(\mathcal{K};\mathbb{Z})$ induces a circular coordinate. Some of these coordinates can be used to detected cycling dynamics. For example, the coordinate in Fig. 2a is almost constant on the left side of the complex while it maps the right half of the complex surjectively onto the circle. Therefore, a lift of this coordinate changes significantly if and only if the time series "cycles" around the right hole in the complex. In particular, the coordinate can be used to detect cycling around the right hole. Similarly, the coordinate in Fig. 2b can be used to detect cycling around the left hole. However, not all cohomology classes induce coordinates suitable for detecting cycling dynamics. For example, the coordinates in Figs. 3a and 3b are not suited for detecting cycling dynamics since they vary around both holes.

We now explain how dynamically relevant coordinates can be obtained. Intuitively, we want different coordinates to describe different features of the dynamics. Therefore, large changes in different lifted coordinates should occur at disjoint periods of time. To capture this, we define the *correlation* of two lifted coordinates $\hat{\theta}$ and $\hat{\eta}$ as

$$c(\hat{\theta},\hat{\eta}) = \langle |\Delta\hat{\theta}|, |\Delta\hat{\eta}| \rangle \tag{1}$$

where the i-th entry of the vector $\Delta\hat{\theta}$ is the forward finite difference $\hat{\theta}_{i+1} - \hat{\theta}_i$ and $\langle\cdot,\cdot\rangle$ denotes the standard Euclidean inner product. Since we are interested in describing all possible cycling dynamics in the system, we want to find a correlation minimizing basis. For a basis B of $H^1(\mathcal{K};\mathbb{Z})$ we define its *correlation* as

$$I(B) = \sum_{\substack{\alpha,\alpha'\in B \\ \alpha\neq\alpha'}} c(\hat{\theta}_\alpha, \hat{\theta}_{\alpha'}). \tag{2}$$

As an example, we again consider the time series 1a. From Fig. 4b we know that for the first 80 time steps, the series does 3.5 turns around the right hole. Now consider Fig. 5 where the lifted coordinates for the bases $\{\alpha,\beta\}$ and $\{\gamma,\delta\}$ are plotted for the first 80 time steps. The plots indicate that the lifted coordinates in Fig. 5a have a lower correlation than the ones in Fig. 5b. An explicit computation (for all 1000 time steps) yields the values 0.158 and 12.8, respectively, confirming that the preferred basis has lower correlation.

We now search for a basis with minimal correlation. Assuming $\alpha_1,\ldots,\alpha_n$ is any basis for the free group $H^1(\mathcal{K};\mathbb{Z})$, every basis can be written as $A\alpha_1,\ldots,A\alpha_n$ where $A \in \mathrm{GL}_n(\mathbb{Z})$. In order to find a correlation minimizing basis, we search $\mathrm{GL}_n(\mathbb{Z})$, starting with the identity $A := \mathrm{I}$ and recursively applying basis change operations (sums of rows/columns, multiplication of rows/columns with a unit) to A up to a given depth. Of all these bases we return the one with minimal correlation.

This approach works sufficiently well for simple examples. However, since we are only searching a finite subset of $\mathrm{GL}_n(\mathbb{Z})$ we have no guarantee of actually finding a minimizer. A better algorithm for finding a correlation minimal basis is a topic for future work.

Given a quantized time series and a circular coordinate, cycling dynamics can be inferred from changes in a lift of the coordinate. More precisely, we define a quantized time series $\hat{x}$ to be *cycling along* α if there is an interval $[k,\ell]$ where $\hat{\theta}_\alpha$

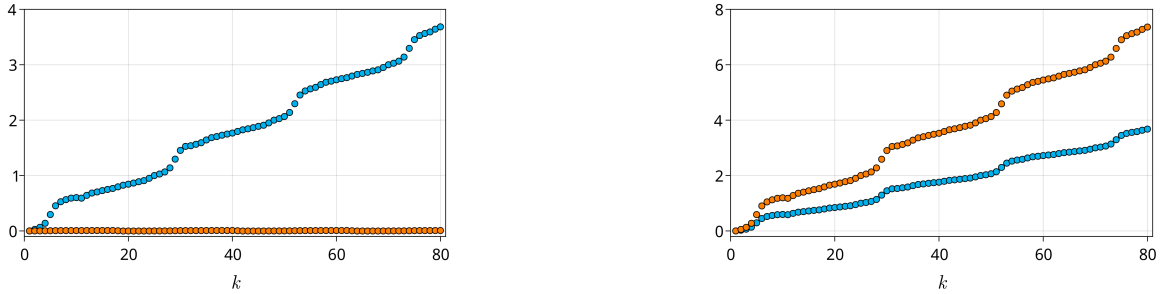

(a) Lift of the coordinates in Fig. 2.

(b) Lift of the coordinates in Fig. 3.

Figure 5: Lifted coordinates for two different bases.

satisfies a *monotonicity criterion* and $|\hat{\theta}_\alpha(\ell) - \hat{\theta}_\alpha(k)| > 1$. The second condition ensures that the time series completes at least one full turn during the segment $[k, \ell]$. The monotonicity criterion we use is the following: Given $\varepsilon > 0$, $\bar{t} \in \mathbb{N}_{>0}$, the lifted coordinate $\hat{\theta} : [0, T] \to \mathbb{R}$ is called $(\varepsilon, \bar{t})$-*increasing along* $[k, \ell]$ if

- $|\theta_\alpha(t + \bar{t}) - \theta_\alpha(t)| > \varepsilon$ for all $t = k, \dots, \ell - \bar{t}$, and
- the sign of $\theta_\alpha(t + \bar{t}) - \theta_\alpha(t)$ is the same for all $t = k, \dots, \ell - \bar{t}$.

For $\bar{t} = 1$, this definition requires $\hat{\theta}_\alpha$ to be monotonic. In practice, it is usually necessary to use $\bar{t} > 1$ due to small back-and-forth movement which decreases the lifted coordinate, or movement orthogonal to the cycling direction which keeps the lifted coordinate constant. Note that the parameters ε and $\bar{t}$ have to be specified by the user; we typically do this by inspecting the lifted coordinates.
We define the subset $E \subset B$ of all *dynamically relevant generators* of a basis B as all $\alpha \in B$ for which the time series is cycling along θ_α. The elements in $B \setminus E$ will be called *spurious* generators.

Macro model for cycling dynamics
We transfer the information on cycling motion back to the cubical covering: A cube ξ in the covering $\mathcal{X}$ is α-*cycling* if the time series is cycling along α on some interval $[k, \ell]$ and there is $j \in [k, \ell]$ such that $\hat{x}_j \in \xi$. For $\xi \in \mathcal{X}$, let $E(\xi) \subset E$ be the set of all dynamically relevant generators α for which ξ is α-cycling.
The cubical covering $\mathcal{X}$ can now be decomposed into equivalence classes: Two cubes are equivalent if they are cycling with respect to the same set of non-spurious generators of $H^1(\mathcal{K}; \mathbb{Z})$:

$$\xi \sim_1 \xi' \iff E(\xi) = E(\xi').$$

We can furthermore distinguish cubes in which the trajectory ceases to be cycling. For this, assume the time series is α-cycling along an interval $[k, \ell]$ which is maximal in the sense that the time series is not α-cycling on any interval which contains $[k, \ell]$. Now let $t \in [k, \ell]$ be the first time step such that $|\hat{\theta}_\alpha(\ell) - \hat{\theta}_\alpha(t)| < 1$. Then the cubes $Q^{-1}(\hat{x}_t), \dots, Q^{-1}(\hat{x}_\ell)$ are precisely those cubes which are hit during the "last full turn" with respect to α in $[k, \ell]$. We call such cubes α-*transient*. For a given cube ξ, we let $E_t(\xi)$ denote the set of all generators which ξ is transient for. As a finer classification of cubes we define

$$\xi \sim_2 \xi' \iff E(\xi) = E(\xi') \text{ and } E_t(\xi) = E_t(\xi').$$

We now classify the cubes in $\mathcal{X}$ according to either of these two equivalence relations and count transitions between the classes. That is, we build the quotient

$$[\mathcal{X}] := \mathcal{X}/\sim = \{[\xi_1]_\sim, \dots, [\xi_T]_\sim\}$$

as well as the transition matrix

$$P(\sim) = (p_{ij}), \quad p_{ij} = \#\{t \in [1, T] \mid \hat{x}_{t-1} \in [\xi_j]_\sim, \hat{x}_t \in [\xi_i]_\sim\}.$$

We now call $(\mathcal{X}/\sim_1, P(\sim_1))$ a macro model, and $(\mathcal{X}/\sim_2, P(\sim_2))$ an extended macro model for the given time series. Figs. 6 and 7 show both macro models for the time series in Fig. 1a.

Experiments

The following results are obtained using our implementation of the pipeline in Section in the programming language Julia [2]. In particular, we use the algorithm in [8] for computing H^1 with integer coefficients.

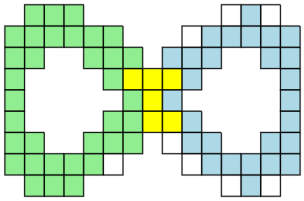

(a) Decomposition.

1157		86	142	α-cyc
	1367	69	6	β-cyc
113	68	134		α-cyc β-cyc
115	6	27		no cycling

(b) Transition matrix.

Figure 6: Macro model for the double well system.

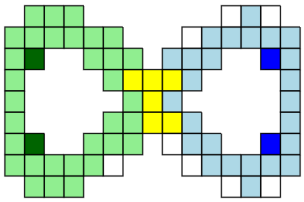

(a) Decomposition.

	10					α-cyc
10	1137			86	142	α-trn
			13			β-cyc
		13	1341	69	6	β-trn
	113		68	134		α-trn β-trn
	115		6	27		no cycling

(b) Transition matrix.

Figure 7: Extended macro model for the double well system.

Perturbed double well

The time series in Fig. 1, which was used to illustrate the constructions in the previous section, was obtained by integrating a stochastically perturbed version of the double well Hamiltonian system

$$dx = f(x)dt + \sigma dB, \tag{3}$$

with $x = (q, p)$, $f(x) = (p, q - q^3)$, $\sigma = (0, 0.025)$ and B denoting Brownian motion. We integrate (3) from the initial value $x = (1, 0.7)$ by the SRIW1 scheme [13] with step size 0.01.

The macro models in Fig. 6 and Fig. 7 were generated using the coordinates in Fig. 2 and the monotonicity criterion "θ is $(0.02, 2)$-increasing". These models are as we would expect for such simple dynamics. The yellow boxes capture the location in phase space where direct transition between loops is possible and the green and blue boxes capture the location where the trajectory cycles around the natural holes.

The Lorenz system

For this example we generated a time series by integrating the Lorenz system with the classical parameters $\sigma = 10$, $\beta = \frac{8}{3}$ and $\rho = 28$ with time step size 0.1 for 1 million time steps using the classical fourth order Runge Kutta method. As starting value, we choose $(0, 10, 0)$, but we discard the first 6000 time steps since they 'close up' the left holes of the complex. This highlights one shortcoming of our current technique which will be addressed in future work.

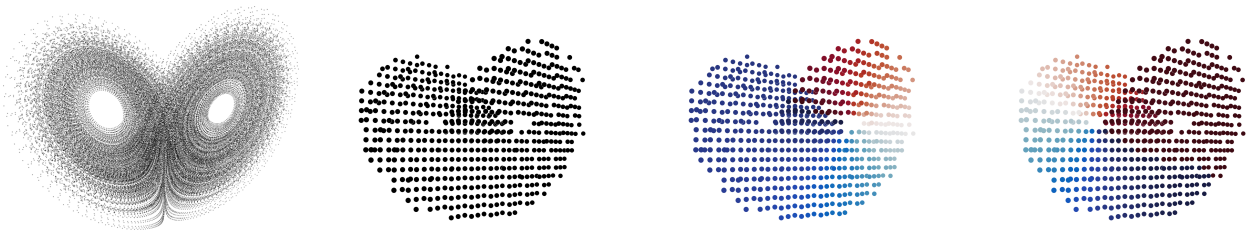

(a) Sampled trajectory. (b) Quantization. (c) Coordinate θ_α. (d) Coordinate θ_β.

Figure 8: Illustration of the pipeline for a trajectory on the Lorenz attractor.

We choose the quantization radius $r = 2.5$ and obtain a Vietoris-Rips complex with two-dimensional first cohomology. We use the monotonicity criterion "θ is $(0.02, 6)$-increasing" for both coordinates. Plots of the time series, the quantized point cloud as well as the coordiantes of the correlation minimizing basis are shown in Fig. 8.

The macro model shown in Fig. 9 nicely captures many important aspects of the dynamics on the Lorenz attractor. We learn that there are (at least) two different types of cycling motion, that each of these occurs in a distinct region in phase space (the blue and green regions), and that these regions intersect (yellow region). We furthermore see that cycling dynamics are present everywhere in the box decomposition since there are no non-cycling boxes.

In the extended macro model (Fig. 10), we see that the cycling regions are subdivided into a cycling set near the center of the wings and a transient set near the outside of the wings. This indicates that all cycling dynamics in the inside of

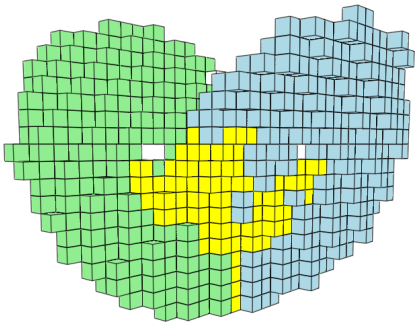

(a) Decomposition.

12060		1042	α-cyc
	12677	901	β-cyc
1043	901	14219	α-cyc β-cyc

(b) Transition matrix.

Figure 9: Macro model for the Lorenz system.

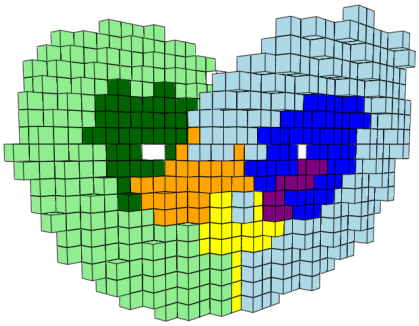

(a) Decomposition.

3046	724			53	305	301	α-cyc
755	7535			37	346		α-trn
		3359	656	128	234	100	β-cyc
		766	7896	30	74	335	β-trn
80	368	9	384	5179	275	904	α-trn β-trn
212	17	229	165	642	3663	5	α-trn β-cyc
336	30	114		1129	36	2386	α-cyc β-trn

(b) Transition matrix.

Figure 10: Extended macro model for the Lorenz system.

the wings eventually moves to the outer regions. The extended model furthermore identifies the regions where direct transitions between cycling dynamics can occur. The purple and yellow regions in Fig. 10a are the only regions where a direct transition from α- to β-cycling dynamics is possible and the orange and yellow regions are the only places that can contain the reverse transition.

Discussion

The techniques described in this paper appear to be a promising novel approach to identifying from time series data regions of phase space in which oscillations occur and locations at which transitions between these oscillations occur. However, a number of distinct questions need to be answered to obtain confidence in applying this technique to complicated higher-dimensional systems, where the results cannot be inspected and modified by visualization. We briefly address those in the following paragraphs.

Construction of the complex. The computation of circle-valued coordinates from data requires the construction of a geometric complex. The approach chosen in this article accomplishes this by constructing a Vietoris–Rips complex from a suitably quantized version of the given time series. In particular, we rely on finding a quantization radius r which is small enough to contain those holes which give rise to dynamically relevant coordinates and large enough to connect the data in a meaningful way. In general, such a radius need not exist. This even happens in the Lorenz system with a trajectory that starts very close to the center of one of the wings.

Finding optimal coordinates. When searching for dynamically relevant coordinates, we encounter the problem of finding a correlation minimizing basis. This poses the natural question of existence and uniqueness of such a basis. In addition, an algorithm is needed to compute this basis or a suitable approximation. Furthermore, even the computation of an arbitrary basis for $H^1(\,\cdot\,;\mathbb{Z})$ is currently not as efficient as we would like. We hope to address this using techniques inspired by those for the computation of (persistent) cohomology with coefficients in a finite field [3].

Identifying cycling motion. In this contribution, cycling motion is identified by analyzing the monotonicity behavior of circular coordinates. While this leads to satisfactory results in the presented examples, we have no general reliable procedure of identifying recurrence. For example, a cycling time series with a bit of back-and-forth movement in every full turn would be difficult to identify using the presented methods.

Appendix: Background

Simplicial complexes. Let V be a finite set. An *(abstract) simplicial complex* with base set V is a subset $\mathcal{K}$ of the power set of V which is closed under the subset relation, i.e. $\sigma \in \mathcal{K}$ implies $\tau \in \mathcal{K}$ for every subset τ of σ. A $\sigma \in \mathcal{K}$ is called a *simplex*, or more precisely a *k-simplex*, where $k = |\sigma| - 1$; the set of k-simplices is denoted by $\mathcal{K}^{(k)}$. In the special cases $k = 0$, 1 or 2 we call σ a vertex, an edge or a triangle, respectively.
Given a finite set $V \subset \mathbb{R}^n$, a metric d on $\mathbb{R}^n$ and a simplex $\sigma \subset V$, the diameter of a simplex is defined as $\operatorname{diam}\sigma = \max_{v,w\in\sigma} d(v,w)$. The simplicial complex $\mathrm{VR}(V,d,r) = \{\sigma \subset V \mid \operatorname{diam}\sigma \leq r\}$ is called the *Vietoris–Rips complex* of V at scale r.

Cochain groups. A *basis* for an abelian group G is a set $(g_i)_{i\in I}$ of elements such that every $g \in G$ can be written uniquely as a finite sum $g = \sum n_j g_j$ with $n_j \in \mathbb{Z}$. An abelian group with a basis is called *free*.
The cochain groups of a simplicial complex are the free abelian groups

$$C^k(\mathcal{K};\mathbb{Z}) = \{\text{functions } \mathcal{K}^{(k)} \to \mathbb{Z}\}$$

where a basis for each group is given by the functions which are 1 on one simplex and 0 on all others.

First Cohomology. Fix a total order on V. We write $[v_0, v_1, \ldots, v_k]$ for a subset $\{v_0, v_1, \ldots, v_k\}$ of V if $v_0 < v_1 < \cdots < v_k$. Clearly, for every $\sigma \in \mathcal{K}$ there are unique $v_0, \ldots, v_k \in V$ such that $\sigma = [v_0, v_1, \ldots, v_k]$.
We define coboundary maps $d_0 : C^0(\mathcal{K};\mathbb{Z}) \to C^1(\mathcal{K};\mathbb{Z})$ and $d_1 : C^1(\mathcal{K};\mathbb{Z}) \to C^2(\mathcal{K};\mathbb{Z})$

$$\begin{aligned}(d_0 f)([v_0,v_1]) &= f(v_1) - f(v_0)\\ (d_1\alpha)([v_0,v_1,v_2]) &= \alpha([v_1,v_2]) - \alpha([v_0,v_2]) + \alpha([v_0,v_1])\end{aligned}$$

Elements in $\ker d_1$ are called *cocycles*, elements in $\operatorname{im} d_0$ *coboundaries*. A calculation shows that $d_1 d_0 = 0$ and therefore $\operatorname{im} d_0 \subset \ker d_1$. We can therefore define the *first cohomology group* as the quotient

$$H^1(\mathcal{K};\mathbb{Z}) = \ker d_1 / \operatorname{im} d_0.$$

It follows from the universal coefficient theorem for cohomology (see section 3.1 of [15]) that $H^1(\mathcal{K};\mathbb{Z})$ is again a free abelian group.

Acknowledgement

The authors thank the DFG for their support via the SFB/TR109 Discretization in Geometry and Dynamics.

References

[1] H. Ban and W. D. Kalies. A computational approach to Conley's decomposition theorem. *J. Comp. Nonl. Dyn.*, 1(4):312–319, 2006.

[2] J. Bezanson, A. Edelman, S. Karpinski, and V. B. Shah. Julia: A Fresh Approach to Numerical Computing. *SIAM Review*, 59: 65–98, 2017.

[3] U. Bauer. Ripser: efficient computation of Vietoris–Rips persistence barcodes. J Appl. and Comput. Topology 5, 391–423 (2021).

[4] C. Conley. *Isolated invariant sets and the Morse index*, volume 38 of *CBMS Regional Conference Series in Mathematics*. American Mathematical Society, Providence, R.I., 1978.

[5] V. de Silva, D. Morozov, and M. Vejdemo-Johansson. Persistent Cohomology and Circular Coordinates. *Discr. Comp. Geom.*, 45(4):737–759, 2009.

[6] M. Dellnitz and O. Junge. On the approximation of complicated dynamical behavior. *SIAM J. Numer. Anal.*, 36(2):491–515, 1999.

[7] M. Dellnitz, O. Junge. Set oriented numerical methods for dynamical systems, B. Fiedler, G. Iooss and N. Kopell (eds.), in: Handbook of Dynamical Systems III: Towards Applications. *World Scientific*, 2002.

[8] S. Harker, K. Mischaikow, M. Mrozek, and V. Nanda. Discrete Morse theoretic algorithms for computing homology of complexes and maps. *Found. Comput. Math.*, 14(1):151–184, 2014.

[9] K. Mischaikow. Topological techniques for efficient rigorous computation in dynamics. *Acta Numer.*, 11:435–477, 2002.

[10] W. D. Kalies, K. Mischaikow, and Vandervorst, R. C. A. M. An algorithmic approach to chain recurrence. *Found. Comput. Math.*, 5(4):409–449, 2005.

[11] K. Mischaikow, M. Mrozek, and F. Weilandt. Discretization strategies for computing Conley indices and Morse decompositions of flows. *J. Comput. Dyn.*, 3(1):1–16, 2016.

[12] G. Osipenko. Construction of attractors and filtrations. In *Conley index theory (Warsaw, 1997)*, volume 47 of *Banach Center Publ.*, pages 173–192. Polish Acad. Sci. Inst. Math., Warsaw, 1999.

[13] A. Rößler. Runge-Kutta methods for the strong approximation of solutions of stochastic differential equations. *SIAM J. Numer. Anal.*, 48(3):922–952, 2010.

[14] P. Skraba, V. de Silva, and M. Vejdemo-Johansson. Topological Analysis of Recurrent Systems. Presented at the NIPS 2012 Workshop on Algebraic Topology and Machine Learning, December 8th, Lake Tahoe, Nevada.

[15] A. Hatcher. Algebraic Topology. Cambridge University Press, Cambridge, 2002